IEEE Open Journal of
Vehicular Technology

Received 12 September 2023; accepted 27 October 2023. Date of publication 1 November 2023;
date of current version 29 November 2023. The review of this article was coordinated by Editor Wen Chen.

Digital Object Identifier 10.1109/OJVT.2023.3329418

A Unified Analysis of Fox H-Fading With Beam Misalignment: Theory and Applications

HUGERLES S. SILVA [1,2] (Member, IEEE), WAMBERTO J. L. QUEIROZ [3], FELIPE A. P. FIGUEIREDO [4] (Member, IEEE), RAUSLEY A. A. DE SOUZA [4,5] (Senior Member, IEEE), AND YONGHUI LI [5] (Fellow, IEEE)

[1]Instituto de Telecomunicações and Departamento de Eletrónica, Telecomunicações e Informática, Universidade de Aveiro, Campus Universitário de Santiago, 3810-193 Aveiro, Portugal
[2]Department of Electrical Engineering, University of Brasília (UnB), Brasília 70910-900, Brazil
[3]Department of Electrical Engineering, Federal University of Campina Grande, Campina Grande 58428-830, Brazil
[4]National Institute of Telecommunications (Inatel), Santa Rita do Sapucaí 37540-000, Brazil
[5]School of Electrical and Information Engineering, The University of Sydney, Sydney, NSW 2006, Australia

CORRESPONDING AUTHOR: Hugerles S. Silva (e-mail: hugerles.silva@av.it.pt).

This work was supported in part by CNPq under Grants 311470/2021-1 and 403827/2021-3, in part by São Paulo Research Foundation (FAPESP) under Grant 2021/06946-0, in part by RNP, with resources from MCTIC, under Grant 01245.020548/2021-07, through the Brazil 6G Project of the Radiocommunication Reference Center (Centro de Referência em Radiocomunicações - CRR) of the National Institute of Telecommunications (Instituto Nacional de Telecomunicações - Inatel), Brazil, in part by Huawei, throguh the Project Advanced Academic Education in Telecommunications Networks and Systems, Contract PPA6001BRA23032110257684, and in part by FCT/MCTES through National Funds and, when applicable, co-funded by EU funds through the Project UIDB/50008/2020-UIDP/50008/2020.

ABSTRACT This paper presents a unified analysis of the Fox H-fading channel with beam misalignment. A statistical framework is introduced that includes new expressions for the probability density function, cumulative distribution function, higher-order moments of the envelope/instantaneous signal-to-noise ratio (SNR), and moment generating function of the instantaneous SNR. The analysis also derives expressions for important metrics such as the bit error probability, outage probability, and ergodic channel capacity, as well as an asymptotic analysis of these metrics. Moreover, this work investigates several special cases and provides a detailed examination of the relationship between the Nakagami-m, α-$\mathcal{F}$, and extended generalized-K fading models and the Fox H-fading distribution. As a result, this analysis facilitates an understanding of how existing work in the literature can be obtained as particular cases of this study. Furthermore, Monte Carlo simulations are conducted to corroborate several curves for different values that characterize the channel and beam misalignment parameters. This presentation helps to extend our understanding of the behavior of the Fox H-fading channel under beam misalignment, which has potential applications in wireless communications and other fields.

INDEX TERMS Beam misalignment, Fox H-fading distribution, unified analysis.

I. INTRODUCTION

In the literature, several works have been presented regarding the misalignment between the transmitting and receiving beams, which results in pointing errors in the transmission systems [1]. Over the years, the misalignment has been studied in different scenarios and, currently, some papers have analyzed the mentioned effect in very important modern applications, such as free space optics (FSO) [2], terahertz (THz) [3], [4] and reconfigurable intelligent surfaces (RIS)-assisted [5], [6] wireless systems. In the mentioned articles, simple or generalist models have been considered to characterize small or large-scale fading. Composite distributions have also been adopted to model environments where multipath coexists with shadowing.

In this article, a statistical framework is presented, and the Fox H-distribution [7] is adopted in order to characterize the multipath fading. The Fox H-function has a compact notation and is generalist [7]. In fact, many continuous probability distributions can be written as special cases of the Fox H-function [8], i.e., a lot of distributions can be written in terms of it (see [9, Table IV]). The mentioned function also has the advantage of allowing a simple derivation of asymptotic expansions for many performance metrics [8]. The asymptotic expansions are important to provide insights into the effect of the channel and beam misalignment parameters on the system performance.

In our work, a unified analysis of Fox H-fading channel with beam misalignment is performed, in which several statistics are deduced. The statistics obtained can be used to derive performance metrics for assessing the performance of wireless communication systems in many scenarios. To the best of the authors' knowledge, no work deals with the Fox H-fading distribution with misalignment. Since the Fox H-distribution is generalist, many works previously presented in the technical literature can be found as particular cases of the studies carried out in this paper. This evidences the usefulness and capability of the Fox H-distribution. In our work, a relationship between the Nakagami-m, α-$\mathcal{F}$, and extended generalized-K (EGK) fading models, and the Fox H-distribution is presented.

The main contributions of this article are:

- A novel unified statistical framework based on the Fox H-fading channel taking beam misalignment into consideration is derived and employed to obtain the probability density function (PDF), cumulative distribution function (CDF), and high-order moments of the received instantaneous signal-to-noise ratio (SNR) and the channel's envelope;
- Derivation of novel unified analytical expressions for the average bit error probability (ABEP), outage probability (OP), and average ergodic channel capacity;
- Accurate asymptotic expressions for the performance metrics aforementioned are derived, giving more understanding of the impact of pointing errors (i.e., misalignment) on the system performance.
- An application concerning cascaded H-fading with beam misalignment channels is provided.

The remainder of the paper is organized as follows. Section II describes the system and channel models adopted. In Section III, a unified analysis is performed for the Fox H-fading channel with pointing errors, and the special cases are analyzed. Section IV presents some performance analyses and their corresponding asymptotic metrics. In Section V, an application in the context of cascaded channels is analyzed. Section VI shows the numerical results and discussions. Section VII brings the conclusions of the paper.

II. SYSTEM AND CHANNEL MODELS

The received signal, at the receiver matched filter output, can be written as

$$Y = h_l H_f H_p X + N, \tag{1}$$

in which X denotes the transmitted signal, N is the additive white Gaussian noise, H_f represents the fading channel, H_p represents the misalignment, and h_l is a constant that represents the path loss.

The fading channel is modeled by the Fox H-distribution, whose PDF of the instantaneous SNR, Γ, is given by [8, Eq. (1)]

$$f_\Gamma(\gamma) = \kappa \mathrm{H}_{p,q}^{m,n}\left(\lambda\gamma \left| \begin{matrix} (a_j, A_j)_{j=1:p} \\ (b_j, B_j)_{j=1:q} \end{matrix} \right.\right), \tag{2}$$

in which $\gamma > 0$, κ and λ are real and positive constants, $\mathrm{H}_{p,q}^{m,n}[\cdot]$ is the Fox H-function [7], and $(x_j, y_j)_{j=1:l} = (x_1, y_1), \ldots, (x_l, y_l)$ are pairs that depend on the adopted fading model. Defining the envelope H_f as the root square of the instantaneous SNR, i.e. $H_f = \sqrt{\Gamma}$, the envelope PDF of the fading can be find from (2) as

$$f_{H_f}(h_f) = \frac{\kappa}{\sqrt{\lambda}} \mathrm{H}_{p,q}^{m,n}\left[\sqrt{\lambda} h_f \left| \begin{matrix} \left(a_j + \frac{A_j}{2}, \frac{A_j}{2}\right)_{j=1:p} \\ \left(b_j + \frac{B_j}{2}, \frac{B_j}{2}\right)_{j=1:q} \end{matrix} \right.\right], \tag{3}$$

$h_f > 0$.

The PDF of the misalignment fading coefficient is given by [2, Eq. (7)]

$$f_{H_p}(h_p) = z^2 A_0^{-z^2} h_p^{z^2-1}, \quad 0 \le h_p \le A_0, \tag{4}$$

in which A_0 is the fraction of the collected power and $z = \omega_{eq}/\sigma$ is the pointing error intensity, defined as the ratio between the equivalent beam radius at the receiver (ω_{eq}) and the pointing error displacement standard deviation σ [10]. For $z \to \infty$, non-pointing error is assumed.

III. A UNIFIED ANALYSIS OF FOX H-FADING WITH BEAM MISALIGNMENT

Lemma III.1 (PDF and CDF of the Instantaneous SNR): Let $\kappa, \lambda, z, A_0, h_l$, and $\gamma \in \mathbb{R}^+$. For the Fox H-fading channel model with beam misalignment, the PDF of the instantaneous SNR Γ is written as

$$f_\Gamma(\gamma) = \frac{\kappa z^2}{2h_l^2 A_0^2} \mathrm{H}_{p+1,q+1}^{m+1,n}\left[\frac{\lambda\gamma}{h_l^2 A_0^2} \left| \begin{matrix} (a_j, A_j)_{j=1:p+1} \\ (b_j, B_j)_{j=1:q+1} \end{matrix} \right.\right], \tag{5}$$

where

$$(a_j, A_j) = \left(z^2/2, 1\right), \quad \text{if } j = p+1 \tag{6}$$

and

$$(b_j, B_j) = \left(z^2/2 - 1, 1\right), \quad \text{if } j = m+1. \tag{7}$$

In turn, the CDF of the instantaneous SNR, Γ, is given by

$$F_\Gamma(\gamma) = \frac{\kappa z^2 \gamma}{2h_l^2 A_0^2} \mathrm{H}_{p+2,q+2}^{m+1,n+1}\left[\frac{\lambda\gamma}{h_l^2 A_0^2} \left| \begin{matrix} (a_j, A_j)_{j=1:p+2} \\ (b_j, B_j)_{j=1:q+2} \end{matrix} \right.\right], \tag{8}$$

in which

$$(a_j, A_j) = \begin{cases} (0, 1), & \text{if } j = n+1 \\ \left(z^2/2, 1\right), & \text{if } j = p+2 \end{cases} \tag{9}$$

and

$$(b_j, B_j) = \begin{cases} \left(z^2/2 - 1, 1\right), & \text{if } j = m+1 \\ (-1, 1), & \text{if } j = q+2 \end{cases}. \tag{10}$$

It is noted that for $j = 1 : m$, $j = 1 : p$ and $j = m+2 : q+1$, the parameters in (5) take the same values as those in (3), respectively, for $j = 1:m$, $j = 1:p$ and $j = m+1:q$. Furthermore, for $j = 1:m$, $j = 1:n$, $j = n+2:p+1$ and $j = m+2:q+1$, the parameters in (8) take the same values as in (3), respectively, for $j = 1:m$, $j = 1:n$, $j = n+1:p$ and $j = m+1:q$.

Proof: See Appendix A. ■

Lemma III.2 (PDF and CDF of the Envelope): Let κ, λ, z, A_0, h_l, and $h \in \mathbb{R}^+$. The PDF of the envelope $H = h_l H_f H_p$, for the Fox H-model with beam misalignment, can be written as

$$f_H(h) = \frac{\kappa z^2 h}{h_l^2 A_0^2} \mathrm{H}_{p+1,q+1}^{m+1,n} \left[\frac{\lambda h^2}{h_l^2 A_0^2} \middle| \begin{matrix} (a_j, A_j)_{j=1:p+1} \\ (b_j, B_j)_{j=1:q+1} \end{matrix} \right], \quad (11)$$

with

$$(a_j, A_j) = \left(z^2/2, 1\right), \quad \text{if } j = p+1, \quad (12)$$

and

$$(b_j, B_j) = \left(z^2/2 - 1, 1\right), \quad \text{if } j = m+1. \quad (13)$$

In turn, the CDF of the envelope, H, is given by

$$F_H(h) = \frac{\kappa z^2 h^2}{2 h_l^2 A_0^2} \mathrm{H}_{p+2,q+2}^{m+1,n+1} \left[\frac{\lambda h^2}{h_l^2 A_0^2} \middle| \begin{matrix} (a_j, A_j)_{j=1:p+2} \\ (b_j, B_j)_{j=1:q+2} \end{matrix} \right], \quad (14)$$

in which

$$(a_j, A_j) = \begin{cases} (0, 1), & \text{if } j = n+1 \\ \left(z^2/2, 1\right), & \text{if } j = p+2 \end{cases} \quad (15)$$

and

$$(b_j, B_j) = \begin{cases} \left(z^2/2 - 1, 1\right), & \text{if } j = m+1 \\ (-1, 1), & \text{if } j = q+2 \end{cases}. \quad (16)$$

It should be mentioned that for $j = 1:m$, $j = 1:p$ and $j = m+2:q+1$, the parameters in (11) take the same values as the parameters in (3), respectively, for $j = 1:m$, $j = 1:p$ and $j = m+1:q$. In addition, for $j = 1:m$, $j = 1:n$, $j = n+2:p+1$ and $j = m+2:q+1$, the parameters in (14) take the same values as the parameters in (3), respectively, for $j = 1:m$, $j = 1:n$, $j = n+1:p$ and $j = m+1:q$.

Proof: See Appendix B. ■

Lemma III.3 (MGF of the Instantaneous SNR): Let κ, λ, z, A_0, s, and $h_l \in \mathbb{R}^+$. The MGF of the instantaneous SNR over the Fox H-model with beam misalignment is given by

$$M_\Gamma(s) = \frac{\kappa z^2}{2\lambda} \times \mathrm{H}_{p+2,q+1}^{m+1,n+1} \left[\frac{\lambda}{h_l^2 A_0^2 (-s)} \middle| \begin{matrix} (a_j + A_j, A_j)_{j=1:p+2} \\ (b_j + B_j, B_j)_{j=1:q+1} \end{matrix} \right], \quad (17)$$

in which

$$(a_j, A_j) = \begin{cases} (0, 1), & \text{if } j = 1 \\ \left(z^2/2, 1\right), & \text{if } j = p+2 \end{cases} \quad (18)$$

and

$$(b_j, B_j) = \left(z^2/2 - 1, 1\right), \quad \text{if } j = m+1. \quad (19)$$

For $j = 1:m$, $j = 2:n+1$, $j = n+2:p+1$ and $j = m+2:q+1$, the parameters in (17) take the same values as the parameters in (3), respectively, for $j = 1:m$, $j = 1:n$, $j = n+1:p$ and $j = m+1:q$.

Proof: See Appendix C. ■

Lemma III.4 (Higher-Order Moments of the Envelope/Instantaneous SNR): For κ, λ, z, A_0, h_l and $\Gamma \in \mathbb{R}^+$ and $k \in \mathbb{N}^+$, the higher-order moments of the instantaneous SNR Γ and envelope H, for the Fox H-model, can be written as

$$\mathbb{E}\left[\Gamma^k\right] = \left(\frac{\kappa z^2}{2 h_l^2 A_0^2}\right) \left(\frac{\lambda}{h_l^2 A_0^2}\right)^{-(k+1)} \Xi(s)\bigg|_{s=k+1} \quad (20)$$

and

$$\mathbb{E}\left[H^k\right] = \left(\frac{\kappa z^2}{2 h_l^2 A_0^2}\right) \left(\frac{\lambda}{h_l^2 A_0^2}\right)^{-(k/2+1)} \Xi(s)\bigg|_{s=k/2+1}, \quad (21)$$

respectively, with

$$\Xi(s) = \frac{\prod_{j=1}^{m} \Gamma(b_j + B_j s) \Gamma\left(\frac{z^2}{2} - 1 + s\right) \prod_{j=1}^{n} \Gamma(1 - a_j - A_j s)}{\prod_{j=n+1}^{p} \Gamma(a_j + A_j s) \Gamma\left(\frac{z^2}{2} + s\right) \prod_{j=m+2}^{q+1} \Gamma(1 - b_j - B_j s)}. \quad (22)$$

For $j = 1:m$, $j = 1:n$, $j = n+1:p$ and $j = m+2:q+1$, the parameters in (22) take the same values as the parameters in (3), respectively, for $j = 1:m$, $j = 1:n$, $j = n+1:p$ and $j = m+1:q$.

Proof: See Appendix D. ■

It is noteworthy to emphasize that the comprehensive analysis presented in this paper, utilizing the Fox H-Fading distribution in the context of beam misalignment, serves as a robust framework. This framework not only encompasses a wide array of distributions previously discussed in the literature but also extends their applicability. In order to evidence this, Table 1 shows the parameter settings from which some useful instantaneous SNR distributions, as for example Nakagami-m, α-$\mathcal{F}$, and extended generalized-K (EGK) fading models can be obtained as particular cases of the instantaneous SNR distribution for the Fox-H fading model considered in this work, as presented in (40). In [9, Table IV], fifteen distributions written in terms of the Fox H-function are presented.

IV. PERFORMANCE METRICS

A. AVERAGE BIT ERROR PROBABILITY

The ABEP under various modulation schemes is given by [11]

$$P_b = \frac{\rho}{2} \sqrt{\frac{\delta}{2\pi}} \int_0^\infty \gamma^{-\frac{1}{2}} \exp\left(-\frac{\delta}{2}\gamma\right) F_\Gamma(\gamma)\, \mathrm{d}\gamma, \quad (23)$$

TABLE I Some Particular Cases

Model	κ	λ	m	n	p	q	(a_j, A_j)	(b_j, B_j)
Nakagami-m	$\frac{m}{\Gamma(m)\bar{\gamma}}$	$\frac{m}{\bar{\gamma}}$	1	0	0	1	–	$(m-1, 1)$
α-$\mathcal{F}$	$\frac{\mu^{\frac{2}{\alpha}}}{\Gamma(\mu)\Gamma(m_s)\bar{\gamma}(m_s-1)^{\frac{2}{\alpha}}}$	$\frac{\mu^{\frac{2}{\alpha}}}{(m_s-1)^{\frac{2}{\alpha}}\bar{\gamma}}$	1	1	1	1	$\left(1-m_s-\frac{2}{\alpha}, \frac{2}{\alpha}\right)$	$\left(\mu-\frac{2}{\alpha}, \frac{2}{\alpha}\right)$
EGK	$\frac{\beta\beta_s}{\Gamma(m_s)\Gamma(m)\bar{\gamma}}$	$\frac{\beta\beta_s}{\bar{\gamma}}$	2	0	0	2	–	$\left(m-\frac{1}{\xi}, \frac{1}{\xi}\right), \left(m_s-\frac{1}{\xi_s}, \frac{1}{\xi_s}\right)$

in which ρ and δ are modulation-dependent parameters (see [11, Table 6.1]).

Replacing (8) into (23), using [7, Eq. (2.19)], [7, Eq. (1.5)] and performing with some simplifications, it follows that

$$P_b = \frac{\rho\kappa z^2}{4\sqrt{\pi}\lambda} \times \mathrm{H}^{m+1,n+2}_{p+3,q+2}\left[\frac{2\lambda}{\delta h_1^2 A_0^2}\middle| \begin{matrix}(\frac{1}{2},1),(a_j+A_j,A_j)_{j=1:p+2}\\ (b_j+B_j,B_j)_{j=1:q+2}\end{matrix}\right]. \tag{24}$$

For $j = 1 : q+2$ and $j = 1 : p+2$, the parameters in (24) take the same values as the parameters in (8).

B. OUTAGE PROBABILITY

The OP is defined as $P_{\text{out}} = F_\Gamma(\gamma_{\text{th}})$, in which γ_{th} is a specified threshold. Using (8),

$$P_{\text{out}} = \frac{\kappa z^2\gamma_{\text{th}}}{2h_1^2A_0^2}\mathrm{H}^{m+1,n+1}_{p+2,q+2}\left[\frac{\lambda\gamma_{\text{th}}}{h_1^2A_0^2}\middle| \begin{matrix}(a_j,A_j)_{j=1:p+2}\\ (b_j,B_j)_{j=1:q+2}\end{matrix}\right]. \tag{25}$$

As P_{out} is given in terms of $F_\Gamma(\gamma)$, the parameters in (25) take the same values as in (8).

C. ERGODIC CHANNEL CAPACITY

The ergodic channel capacity, denoted by C_{erg}, is given by [11]

$$C_{\text{erg}} = \int_0^\infty \log_2(1+\gamma) f_\Gamma(\gamma)\,\mathrm{d}\gamma. \tag{26}$$

Substituting (5) into (26), using [12, id 01.04.26.0003.01], [12, id 07.34.26.0008.01], and [7, Eq. (2.8)], C_{erg} can be written after some simplifications as

$$C_{\text{erg}} = \frac{\kappa z^2}{2h_1^2A_0^2\log(2)}\mathrm{H}^{m+3,n+1}_{p+3,q+3}\left[\frac{\lambda}{h_1^2A_0^2}\middle| \begin{matrix}(a_j,A_j)_{j=1:p+3}\\ (b_j,B_j)_{j=1:q+3}\end{matrix}\right], \tag{27}$$

in which

$$(a_j, A_j) = \begin{cases}(-1,1), & \text{if } j = n+1\\ (z^2/2, 1), & \text{if } j = p+2,\\ (0,1), & \text{if } j = p+3\end{cases} \tag{28}$$

and

$$(b_j, B_j) = \begin{cases}(z^2/2-1, 1), & \text{if } j = m+1\\ (-1,1), & \text{if } j = m+2.\\ (-1,1), & \text{if } j = m+3\end{cases} \tag{29}$$

For $j = 1 : m$, $j = 1 : n$, $j = n+2 : p+1$ and $j = m+4 : q+3$, the parameters in (27) take the same values as in (3), respectively, for $j = 1 : m$, $j = 1 : n$, $j = n+1 : p$ and $j = m+1 : q$.

D. ASYMPTOTIC ANALYSIS

For the asymptotic analysis, it is appropriate to write the Fox H-function in the Mellin-Barnes representation

$$\mathrm{H}^{a,b}_{c,d}\left[v\middle| \begin{matrix}(a_j+A_j,A_j)_{j=1:c}\\ (b_j+B_j,B_j)_{j=1:d}\end{matrix}\right] = \frac{1}{j2\pi}\int_{\mathcal{L}} \mathcal{X}^{a,b}_{c,d}(s) v^{-s} ds, \tag{30}$$

in which $\mathcal{X}^{a,b}_{c,d}(s)$ is equal to

$$\frac{\prod_{i=1}^{a}\Gamma(b_i+B_i+B_is)\prod_{i=1}^{b}\Gamma(1-(a_i+A_i)-A_is)}{\prod_{i=a+1}^{d}\Gamma(1-(b_i+B_i)-B_is)\prod_{j=b+1}^{c}\Gamma(a_i+A_i+A_is)}. \tag{31}$$

In the following analysis, based on [13, Theorem 1.11], the minimum value of the simple poles of $\Gamma(b_i + B_i + B_is)$ for $1 \le i \le a$ depends on of the relationship between z and the parameters that characterize each fading model contemplated by Fox H-distribution.

1) ASYMPTOTIC AVERAGE BIT ERROR PROBABILITY

From (24) and (30), given an index j_0, equal to the value of j for which the sequence of values $s_j = \mathrm{Re}(b_j + B_j)/B_j$, with $1 \le j \le m+1$, takes minimum value, then, according to [13, Theorem 1.11], when $\lambda \to 0$ (or $\bar{\gamma} \to \infty$), the Fox H-function tends asymptotically to $(\lambda/\rho h_1^2A_0^2)^{s_{j_0}} h^\star_{j_0}$, in which $h^\star_{j_0}$ is obtained as [13, Eq. (1.8.5)]

$$h^\star_{j_0} = \frac{1}{B_{j_0}}\mathcal{X}^{m+1,n+2}_{p+3,q+2}\left(-s_{j_0}\right), \tag{32}$$

with $\mathcal{X}^{m+1,n+2}_{p+3,q+2}(\cdot)$ given by (31). In (32), $i \neq j_0$ in the product from $i = 1$ to $m+1$ and the pairs (a_i, A_i) and (b_i, B_i) have the same structure as in (24). Therefore, after some simplifications, the asymptotic ABEP can be written as

$$P_b^\infty = \frac{\rho\kappa z^2}{4\sqrt{\pi}\lambda}\frac{1}{B_{j_0}}\left(\frac{2\lambda}{\delta h_l^2A_0^2}\right)^{s_{j_0}}\mathcal{X}^{m+1,n+2}_{p+3,q+2}(-s_{j_0}). \tag{33}$$

In high SNRs values, $P_b^\infty \sim \bar{\gamma}^{-G_{\text{d}}}$, where G_{d} is the diversity order/gain. It is noted that the diversity order depends on the fading and pointing error parameters.

2) ASYMPTOTIC OUTAGE PROBABILITY

The asymptotic OP can be derived from (25), applying property [7, Eq. (1.5)] and [13, Theorem 1.11]. By proceeding similarly to the derivation of the asymptotic ABEP, P_{out}^{∞} is given, after simplifications, by

$$P_{\text{out}}^{\infty} = \frac{\kappa z^2}{2\lambda}\frac{1}{B_{j_0}}\left(\frac{\lambda\gamma_{\text{th}}}{h_1^2A_0^2}\right)^{s_{j_0}}\mathcal{X}_{p+2,q+2}^{m+1,n+1}(-s_{j_0}), \tag{34}$$

in which j_0 is equal to the value of the integer index j for which the sequence of values $s_j = \text{Re}(b_j + B_j)/B_j$, with $1 \leq j \leq m+1$, takes minimum value. Besides that, $i \neq j_0$ in the product from $i = 1$ to $m+1$, $\mathcal{X}_{p+2,q+2}^{m+1,n+1}(s)$ is given by (31) and the pairs (a_i, A_i) and (b_i, B_i) have the same structure as in (25). In this case, $P_{\text{out}}^{\infty} \sim \bar{\gamma}^{-G_{\text{d}}}$, and G_{d} also depends on the fading and pointing errors parameters.

3) ASYMPTOTIC ERGODIC CHANNEL CAPACITY

The asymptotic ergodic capacity is given by [14]

$$C_{\text{erg}}^{\infty} \approx \log_2(\bar{\gamma}) + \log_2(e)\frac{\partial}{\partial n}\frac{\mathbb{E}[\gamma^n]}{\bar{\gamma}^n}\bigg|_{n=0}, \tag{35}$$

in which $\partial/\partial n$ is the first derivative operator. Replacing (20) in (35) and proceeding with simplifications,

$$C_{\text{erg}}^{\infty} = \log_2\left(\frac{h_1^2A_0^2}{\lambda}\right) + \log_2(e)\left[S + \psi\left(\frac{z^2}{2}\right) - \psi\left(\frac{z^2}{2}+1\right)\right], \tag{36}$$

with $\psi(x) = \Gamma'(x)/\Gamma(x)$ is the digamma function [15, Eq. (8.36)] and

$$S = \sum_{i=1}^{m} B_i\psi(b_i + B_i) + \sum_{i=m+2}^{q+1} B_i\psi(1-(b_i+B_i)) - \sum_{i=1}^{n} A_i\psi(1-(a_i+A_i)) - \sum_{i=n+1}^{p} A_i\psi(a_i+A_i). \tag{37}$$

V. CASCADED H-FADING WITH BEAM MISALIGNMENT CHANNELS

In this section, we apply our framework within the context of cascaded H-fading channels with beam misalignment. The literature is replete with numerous practical applications that draw parallels to cascaded systems or, equivalently, the product of random variables. Noteworthy examples can be found in the domains of multihop THz links [16], RIS [5], and drone communication [17], all of which demonstrate the relevance and versatility of our approach.

Lemma V.1 (OP and Asymptotic OP under Cascaded H-Fading Channels): Let κ_j, λ_j, z_j, A_{0_j}, h_{1_j}, and $\gamma_{\text{th}} \in \mathbb{R}^+$, with $j = 1, 2\cdots, N$. The OP under cascaded Fox H-fading channel model with beam misalignment is given by (38), shown at the bottom of this page, in which each set of $p+1$ pairs (a_j, A_j) and $q+1$ pairs (b_j, B_j) takes values according to the structure in (5) for $j = 1 : p+1$ and $j = 1 : q+1$. Furthermore, $(a_j, A_j) = (0, 1)$ and $(b_j, B_j) = (-1, 1)$ for $j = N(p+1)+1$ and $j = N(q+1)+1$, respectively.

In turn, the asymptotic OP is written as

$$P_{\text{out}}^{\infty} = \frac{1}{B_{j_0}}\prod_{j=1}^{N}\frac{\kappa_j z_j^2}{2\lambda_j}\left(\prod_{j=1}^{N}\frac{\lambda_j\gamma_{\text{th}}}{h_{1_j}^2A_{0_j}^2}\right)^{s_{j_0}} \times \mathcal{X}_{N(p+1)+1,N(q+1)+1}^{N(m+1),Nn+1}(-s_{j_0}). \tag{39}$$

Proof: See Appendix E. ■

VI. NUMERICAL RESULTS

In this section, theoretical curves as a function of the average SNR, $\bar{\gamma} = \mathbb{E}[\Gamma]$, are shown and corroborated by Monte-Carlo simulations under different channel parameters and pointing errors. In our simulations, the Fox H-function implementation available in [18] is considered.

Curves for the average BEP under the binary phase shift keying (BPSK) scheme, OP, and average ergodic channel capacity are presented in Figs. 1, 2, and 3 respectively, for different values of the parameters m and z. Asymptotic curves are also provided. In this work, in order to validate the proposed statistical framework, the Nakagami-m fading model is adopted, whose parameters are shown in Table 1. As a benchmark, the Rayleigh fading model (with $m = 1.0$) is also included. In all evaluated scenarios, the curves are plotted considering weak, moderate, and heavy pointing errors and different severity levels of fading.

Firstly, as observed in the figures, a strong adherence between the theoretical and simulated curves is noticed, which validates the theoretical analysis. For a given average SNR $\bar{\gamma}$, the system performance is improved as the parameters z and/or m increase, i.e., the ABEP and the OP values decrease, and the capacity values increase. As previously defined, z is the ratio between the equivalent beam radius at the receiver and the standard deviation of the random radial shift of the beam relative to the center of the circular region where the beam should be positioned without disturbances, known as pointing error displacement standard deviation. When the variance of this random shift increases, for a Gaussian beam model, the beam power received by the reception antenna

$$P_{\text{out}} = \prod_{j=1}^{N}\frac{\kappa_j z_j^2}{2\lambda_j}\text{H}_{N(p+1)+1,N(q+1)+1}^{N(m+1),Nn+1}\left[\prod_{j=1}^{N}\frac{\lambda_j\gamma_{\text{th}}}{h_{1_j}^2A_{0_j}^2}\middle|\begin{matrix}(a_j+A_j, A_j)_{j=1:N(p+1)+1}\\(b_j+B_j, B_j)_{j=1:N(q+1)+1}\end{matrix}\right] \tag{38}$$

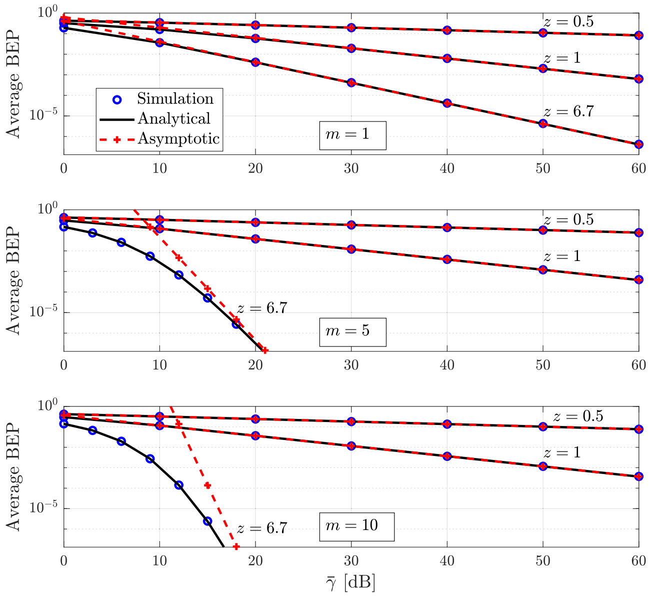

FIGURE 1. Average BEP for BPSK under different severity levels of fading (m) and pointing errors conditions (z), with $h_l = 1$, $A_0 = 0.8$, $\rho = 1$ and $\delta = 0.5$.

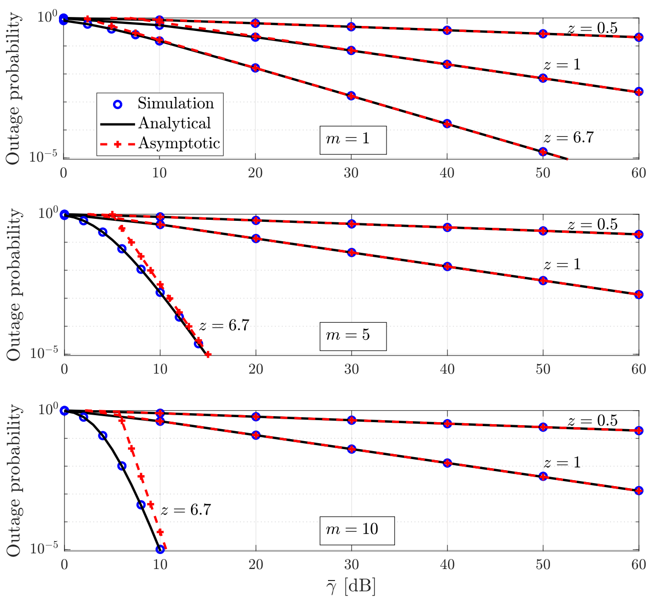

FIGURE 2. Outage probability under different severity levels of fading (m) and pointing errors conditions (z), with $h_l = 1$, $A_0 = 0.8$ and $\gamma_{th} = 0$ dB.

decreases, and all evaluated metrics are directly affected, as can be seen in all curves. For lower values of z, which mimics a heavy pointing errors condition, such as 0.5, it is noted that the parameter m, that characterizes the Nakagami fading intensity, has almost no impact on the metrics. The slope of asymptotic curves changes as z and/or m varies, supporting the idea that the diversity order depends on these parameters.

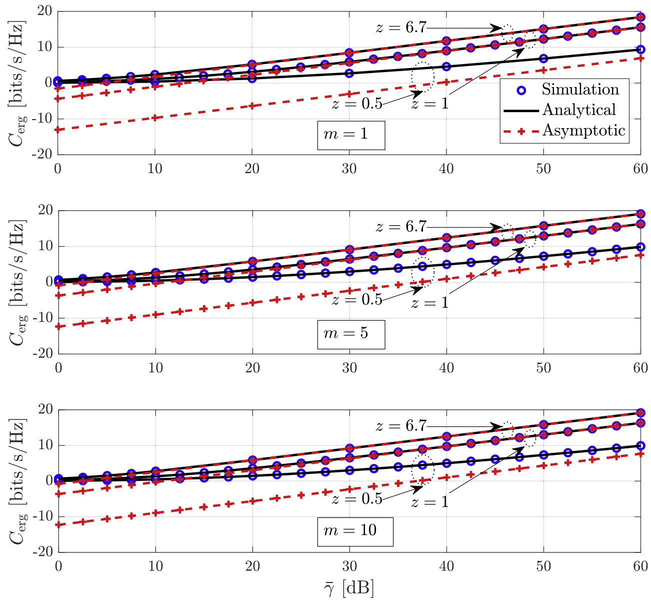

FIGURE 3. Average ergodic channel capacity under different severity levels of fading (m) and pointing error conditions (z), with $h_l = 1$ and $A_0 = 0.8$.

VII. CONCLUSION

In this paper, a unified analysis was presented for the Fox H-fading model with beam misalignment. New expressions were derived for important statistics, such as PDFs, CDFS, higher-order moments, and MGF; as well as for important metrics, such as OP, ABEP, and ergodic channel capacity. Furthermore, simple and accurate asymptotic expressions were obtained for the above-mentioned performance metrics. Several special cases encompassed by the expressions presented in this article were provided. All expressions were corroborated by computational simulations.

APPENDIX

APPENDIX A

Consider $H = h_l H_f H_p$. The PDF of H_f is given by (3) and the PDF of H_p is given by (4). By making the change of variables $\Gamma_f = H_f^2$ and $\Gamma_p = H_p^2$, $f_{\Gamma_f}(\gamma)$ and $f_{\Gamma_p}(\gamma)$ can be written, respectively, as

$$f_{\Gamma_f}(\gamma) = \kappa \mathrm{H}^{m,n}_{p,q}\left[\lambda\gamma \middle| \begin{matrix}(a_j, A_j)_{j=1:p}\\(b_j, B_j)_{j=1:q}\end{matrix}\right], \gamma > 0, \tag{40}$$

and

$$f_{\Gamma_p}(\gamma) = \frac{z^2}{2} A_0^{-z^2} \gamma^{\frac{z^2}{2}-1}, \quad 0 \le \gamma \le A_0^2. \tag{41}$$

Denote $Y = \Gamma_f \Gamma_p$. Thus, the PDF of Y can be calculated as

$$f_Y(y) = \int_{-\infty}^{\infty} \frac{1}{|x|} f_{\Gamma_f}\left(\frac{y}{x}\right) f_{\Gamma_p}(x) \mathrm{d}x. \tag{42}$$

Replacing (40) and (41) in (42), expressing the Fox H-function in terms of the Mellin-Barnes integral and changing the integration order, the resulting integrand is a simple power, and the integral can be easily solved. Using [12, id

06.05.17.0002.01], [7, Eq. (1.2)] and proceeding with some simplifications, the PDF of Y is given by

$$f_Y(y) = \frac{\kappa z^2}{2A_0^2} \mathrm{H}_{p+1,q+1}^{m+1,n}\left[\frac{\lambda y}{A_0^2}\middle|\begin{matrix}(a_j, A_j)_{j=1:p+1}\\(b_j, B_j)_{j=1:q+1}\end{matrix}\right], \quad (43)$$

in which

$$(a_j, A_j) = \left(z^2/2, 1\right), \quad \text{if } j = p+1 \quad (44)$$

and

$$(b_j, B_j) = \left(z^2/2 - 1, 1\right), \quad \text{if } j = m+1. \quad (45)$$

For $j = 1 : m$, $j = 1 : p$ and $j = m+2 : q+1$, the parameters in (43) take the same values as in (3), respectively, for $j = 1 : m$, $j = 1 : p$ and $j = m+1 : q$.

By making $\Gamma = h_1^2 Y$, it follows that

$$f_\Gamma(\gamma) = \frac{1}{h_1^2} f_Y\left(\frac{\gamma}{h_1^2}\right). \quad (46)$$

Substituting (43) in (46), (5) is easily obtained.

The CDF of the instantaneous SNR, $F_\Gamma(\gamma)$, is calculated as $F_\Gamma(\gamma) = \int_0^\gamma f_\Gamma(v)\mathrm{d}v$. Using (5) and steps similar to deriving the PDF from instantaneous SNR, (8) is obtained. This completes the proof.

APPENDIX B

By making $\Gamma = H^2$, it follows that $f_H(h) = 2h f_\Gamma(h^2)$. By using (5), (11) is deduced. Furthermore, the CDF $F_H(h)$ is given by $F_H(h) = \int_0^h f_H(v)\mathrm{d}v$. Writing the Fox H-function in terms of the Mellin-Barnes integral, using [12, id 06.05.17.0002.01], [7, Eq. (1.2)] and making some simplifications, (14) is derived, that completes the proof.

APPENDIX C

The MGF of the instantaneous SNR, $\mathrm{M}_\Gamma(s)$, is calculated as $\mathcal{L}\{f_\Gamma(\gamma)\}(-s)$, in which $\mathcal{L}\{\cdot\}$ represents the Laplace transform. Therefore

$$\mathrm{M}_\Gamma(s) = \int_0^\infty f_\Gamma(\gamma)\exp(-s\gamma)\,\mathrm{d}\gamma\bigg|_{(-s)}. \quad (47)$$

Replacing (5) in (47), using [7, Eq. (2.19)], [7, Eq. (1.5)] and performing with some simplifications, (17) is obtained, that completes the proof.

APPENDIX D

The higher-order moments of the envelope/instantaneous SNR are given by $\mathbb{E}[X^k] = \int_0^\infty x^k f_X(x)\mathrm{d}x$, in which $f_X(x)$ denotes the PDF of the envelope H or the instantaneous SNR Γ. Plugging (5) or (11) in the previous expression of $\mathbb{E}[X^k]$ and using [7, Eq. (2.9)], (20) or (21) can be deduced after simplifications. Thus, the proof is complete.

APPENDIX E

In cascaded channels, $\Gamma = \Gamma_1\Gamma_2\cdots\Gamma_N$. Using [19, Eq. (2.9)] and knowing that $f_{\Gamma_j}(\gamma_j)$, with $j = 1, 2, \ldots, N$, is given by (5), then it is possible to derive an expression for $\mathcal{M}\{f_\Gamma(\gamma)\} = \prod_{j=1}^N \mathcal{M}\{f_{\Gamma_j}(\gamma)\}$ where $\mathcal{M}\{\cdot\}$ is the Merllin transform, as

$$\mathcal{M}\{f_\Gamma(\gamma)\} = \prod_{j=1}^N \frac{\kappa_j z_j^2}{2h_{1_j}^2 A_{0_j}^2}\left(\prod_{j=1}^N \frac{h_{1_j}^2 A_{0_j}^2}{\lambda_j}\right)^s \times \frac{\prod_{j=1}^{N(m+1)}\Gamma(b_j + B_j s)\prod_{j=1}^{Nn}\Gamma(1 - a_j - A_j s)}{\prod_{j=Nn+1}^{N(p+1)}\Gamma(a_j + A_j s)\prod_{j=N(m+1)+1}^{N(q+1)}\Gamma(1 - b_j - B_j s)}. \quad (48)$$

Using [19, Eq. (3.2)], $f_\Gamma(\gamma)$ is given by

$$f_\Gamma(\gamma) = \prod_{j=1}^N \frac{\kappa_j z_j^2}{2h_{1_j}^2 A_{0_j}^2} \times \mathrm{H}_{N(p+1),N(q+1)}^{N(m+1),Nn}\left[\prod_{j=1}^N \frac{\lambda_j \gamma}{h_{1_j}^2 A_{0_j}^2}\middle|\begin{matrix}(a_j, A_j)_{j=1:N(p+1)}\\(b_j, B_j)_{j=1:N(q+1)}\end{matrix}\right]. \quad (49)$$

Integrating (49), knowing that $\int_0^\gamma x^{n-1}\mathrm{d}x = \gamma^n/n$, $\Gamma(\gamma+1) = \gamma\Gamma(\gamma)$, using [7, Eq. (1.60)] and making $\gamma = \gamma_{\text{th}}$, (38) is obtained. Proceeding with similar steps as presented in Section IV.D, the asymptotic OP is derived. Hence, the proof is concluded.

REFERENCES

[1] A. A. Boulogeorgos, E. N. Papasotiriou, and A. Alexiou, "Analytical performance assessment of THz wireless systems," *IEEE Access*, vol. 7, pp. 11436–11453, 2019.

[2] O. S. Badarneh, R. Derbas, F. S. Almehmadi, F. E. Bouanani, and S. Muhaidat, "Performance analysis of FSO communications over $\mathcal{F}$ turbulence channels with pointing errors," *IEEE Commun. Lett.*, vol. 25, no. 3, pp. 926–930, Mar. 2021.

[3] O. S. Badarneh, "Performance analysis of terahertz communications in random fog conditions with misalignment," *IEEE Wireless Commun. Lett.*, vol. 11, no. 5, 962–966, May 2022.

[4] A. A. Boulogeorgos, J. M. Riera, and A. Alexiou, "On the joint effect of rain and beam misalignment in terahertz wireless systems," *IEEE Access*, vol. 10, pp. 58997–59012, 2022.

[5] A. A. Boulogeorgos, N. D. Chatzidiamantis, H. G. Sandalidis, A. Alexiou, and M. D. Renzo, "Cascaded composite turbulence and misalignment: Statistical characterization and applications to reconfigurable intelligent surface-empowered wireless systems," *IEEE Trans. Veh. Technol.*, vol. 71, no. 4, pp. 3821–3836, Apr. 2022.

[6] V. K. Chapala and S. M. Zafaruddin, "Exact analysis of RIS-aided THz wireless systems over α-μ fading with pointing errors," *IEEE Internet Things J.*, vol. 9, no. 14, pp. 3508–3512, Jul. 2022.

[7] A. M. Mathai, R. K. Saxena, and H. J. Haubold, *The H-Function: Theory and Applications*. New York, NY, USA: Springer, 2009.

[8] H. R. Alhennawi, M. M. H. E. Ayadi, M. H. Ismail, and H. -A. M. Mourad, "Closed-form exact and asymptotic expressions for the symbol error rate and capacity of the H-function fading channel," *IEEE Trans. Veh. Technol.*, vol. 65, no. 4, pp. 1957–1974, Apr. 2016.

[9] P. S. Chauhan, S. Kumar, A. Jain, and L. Hanzo, "An asymptotic framework for Fox's H-fading channel with application to diversity-combining receivers," *IEEE Open J. Veh. Technol.*, vol. 4, pp. 404–416, 2023.

[10] I. S. Ansari, F. Yilmaz, and M. -S. Alouini, "Performance analysis of free-space optical links over málaga ($\mathcal{M}$) turbulence channels with pointing errors," *IEEE Trans. Wireless Commun.*, vol. 15, no. 1, pp. 91–102, Jan. 2016.

[11] A. Goldsmith, *Wireless Communication*. Cambridge, U.K.: Cambridge Univ. Press, 2005.

[12] Wolfram Research, Inc., "Wolfram research," 2020. Accessed: Mar. 16, 2022. [Online]. Available: http://functions.wolfram.com/id

[13] A. A. Kilbas and M. Saigo, *H-Transforms: Theory and Applications*. Boca Raton, FL, USA: CRC Press Inc., 2004.

[14] F. Yilmaz and M. S. Alouini, "Novel asymptotic results on the high-order statistics of the channel capacity over generalized fading channels," in *Proc. IEEE Int. Workshop Signal Process. Adv. Wireless Commun.*, 2012, pp. 389–393.

[15] I. S. Gradshteyn and I. M. Ryzhik, *Table of Integrals, Series and Products*. New York, NY, USA: Academic Express, 2007.

[16] P. Bhardwaj and S. M. Zafaruddin, "On the performance of multi-hop THz wireless system over mixed channel fading with shadowing and antenna misalignment," *IEEE Trans. Commun.*, vol. 70, no. 11, pp. 7748–7763, Nov. 2022.

[17] O. A. Amodu, C. Jarray, S. A. Busari, and M. Othman, "THz-enabled UAV communications: Motivations, results, applications, challenges, and future considerations," *Ad Hoc Netw.*, vol. 140, no. 1, pp. 1–17, Mar. 2023.

[18] A. Soulimania, M. Benjillalia, H. Chergui, and D. B. d. Costa, "Multihop Weibull-fading communications: Performance analysis framework and applications," *J. Franklin Inst.*, vol. 358, no. 15, pp. 1–35, Aug. 2021.

[19] M. D. Springer and W. E. Thompson, "The distribution of products of independent random variables," *SIAM J. Appl. Math.*, vol. 14, no. 3, pp. 511–526, May 1966.

HUGERLES S. SILVA (Member, IEEE) received the B.Sc., M.Sc., and Ph.D. degrees in electrical engineering from the Federal University of Campina Grande, Brazil, in 2014, 2016, and 2019, respectively. In 2021, he joined the University of Brasília where is currently a Professor. He is currently a Researcher with the Instituto de Telecomunicações in Portugal. His main research interests include wireless communication, digital signal processing and wireless channel modeling.

WAMBERTO J. L. DE QUEIROZ received the M.Sc. degree in electrical engineering from the Federal University of Paraíba - UFPB, Campina Grande, Brazil, in 2000, and the D.Sc. degree from the Federal University of Campina Grande - UFCG, in 2004. He was an adjunct Professor with Federal University of Ceará - UFC from 2007 to 2010, joined UFCG in 2010 and has been an Associate Professor with UFCG since 2018. His current research interests include digital communications over fading channels, channel modeling and simulations, spectrum sensing systems and estimation theory.

FELIPE A. P. FIGUEIREDO (Member, IEEE) received the B.Sc. and M.Sc. degrees in telecommunication engineering from the National Institute of Telecommunications (Inatel), Brazil, in 2004 and 2011, respectively, and the Ph.D. degree from the State University of Campinas (UNICAMP), Brazil, in 2019 and the second Ph.D. degree from the University of Ghent (UGhent), Belgium, in 2021. He has been working on the research and development of telecommunication systems for more than 15 years. His research interests include digital signal processing, digital communications, mobile communications, MIMO, multicarrier modulations, FPGA development, and machine learning.

RAUSLEY A. A. DE SOUZA (Senior Member, IEEE) received the B.S.E.E. and M.Sc. degrees from the National Institute of Telecommunication (INATEL), Brazil, in 1994 and 2002, respectively, and the Ph.D. degree from the State University of Campinas, Campinas, Brazil, in 2009. Prior to joining the Academy, he worked in industry. In 2002, he joined the INATEL, where he is a Full Professor. His research focuses on wireless communications.

YONGHUI LI (Fellow, IEEE) received the Ph.D. degree from the Beijing University of Aeronautics and Astronautics, Beijing, China, in 2002. Since 2003, he has been with the Centre of Excellence in Telecommunications, the University of Sydney, Camperdown, NSW, Australia. He is currently a Professor and Director of Wireless Engineering Laboratory with the School of Electrical and Information Engineering, University of Sydney. He was the recipient of the Australian Queen Elizabeth II Fellowship in 2008 and the Australian Future Fellowship in 2012. His current research interests are in the area of wireless communications, with a particular focus on MIMO, millimeter wave communications, machine to machine communications, coding techniques and cooperative communications. He holds a number of patents granted and pending in these fields. He was the Editor of IEEE TRANSACTIONS ON COMMUNICATIONS and IEEE TRANSACTIONS ON VEHICULAR TECHNOLOGY. He also was the Guest Editor for several IEEE journals, such as IEEE JOURNAL ON SELECTED AREAS IN COMMUNICATIONS, *IEEE Communications Magazine*, IEEE INTERNET OF THINGS JOURNAL, IEEE ACCESS. He was the recipient of the best paper awards from IEEE International Conference on Communications (ICC) 2014, IEEE PIRMC 2017 and IEEE Wireless Days Conferences (WD) 2014.